THE JOURNAL OF BIOLOGICAL CHEMISTRY VOL. 282, NO. 42, pp. 31038–31045, October 19, 2007

High Glucose Increases Angiopoietin-2 Transcription in Microvascular Endothelial Cells through Methylglyoxal Modification of mSin3A*[S]

Received for publication, June 7, 2007, and in revised form, July 31, 2007 Published, JBC Papers in Press, August 1, 2007, DOI 10.1074/jbc.M704703200

Dachun Yao[‡1], Tetsuya Taguchi[‡1], Takeshi Matsumura[‡], Richard Pestell[§], Diane Edelstein[‡], Ida Giardino[¶], Guntram Suske[‖], Naila Rabbani[**], Paul J. Thornalley[**], Vijay P. Sarthy[‡‡], Hans-Peter Hammes[§§], and Michael Brownlee[‡2]

From the [‡]Juvenile Diabetes Research Foundation International Center for Diabetic Complications Research, Albert Einstein College of Medicine, Bronx, New York 10461, [§]Kimmel Cancer Center, Department of Biochemistry and Molecular Biology, Thomas Jefferson University, Philadelphia, Pennsylvania 19107, [¶]Department of Biomedical Sciences, University of Foggia, Via Pinto 1, 71100 Foggia, Italy, [‖]Institut fuer Molekularbiologie und Tumorforschung, Philipps-Universitaet Marburg, Emil-Mankopff-Strasse 2, D-35037 Marburg, Germany, [**]Protein Damage and Systems Biology Research Group, Warwick Medical School and Systems Biology Centre, Clinical Sciences Research Institute, University of Warwick, Coventry CV2 2DX, United Kingdom, [‡‡]Department of Ophthalmology, Feinberg School of Medicine, Northwestern University, Chicago, Illinois 60093, and [§§] Fifth Medizinische Klinik-Theodor-Kutzer-Ulfer 1-3, University of Mannheim, 68167 Mannheim, Germany

Methylglyoxal is a highly reactive dicarbonyl degradation product formed from triose phosphates during glycolysis. Methylglyoxal forms stable adducts primarily with arginine residues of intracellular proteins. The biologic role of this covalent modification in regulating cell function is not known. Here we report that in mouse kidney endothelial cells, high glucose causes increased methylglyoxal modification of the corepressor mSin3A. Methylglyoxal modification of mSin3A results in increased recruitment of *O*-GlcNAc-transferase, with consequent increased modification of Sp3 by *O*-linked *N*-acetylglucosamine. This modification of Sp3 causes decreased binding to a glucose-responsive GC-box in the angiopoietin-2 (*Ang-2*) promoter, resulting in increased *Ang-2* expression. Increased Ang-2 expression induced by high glucose increased expression of intracellular adhesion molecule 1 and vascular cell adhesion molecule 1 in cells and in kidneys from diabetic mice and sensitized microvascular endothelial cells to the proinflammatory effects of tumor necrosis factor α. This novel mechanism for regulating gene expression may play a role in the pathobiology of diabetic vascular disease.

Methylglyoxal (MG)[3] is a highly reactive α-oxoaldehyde formed in cells primarily from the triose phosphate intermediates of glycolysis, dihydroxyacetone phosphate and glyceraldehyde 3-phosphate (1, 2). It is the major physiologic substrate for the enzyme glyoxalase I, which is encoded by the *GLOI* gene. Together with glyoxalase II and a catalytic amount of glutathione, glyoxalase I reduces methylglyoxal to D-lactate (3). In cells, methylglyoxal reacts almost exclusively with arginine residues to form the major methylglyoxal-derived epitope hydroimidazolone MG-H1 (*Nα*-acetyl-*Nδ* (5-hydro-5-methyl)-4-imidazolone) (4). Changes in methylglyoxal concentration have been implicated in the pathobiology of a variety of important diseases, including diabetic vascular disease.

Diabetes increases levels of the methylglyoxal arginine-derived hydroimidazolone adduct MG-H1 in retina, renal glomerulus, and sciatic nerve of rats (5, 6), and MG-H1 is also increased in aortic endothelial cells cultured in high glucose (7). Diabetes also induces a significant increase in retinal and glomerular expression of angiopoietin-2 (Ang-2) in rats (8–11). In diabetic retinal capillaries, increased Ang-2 is associated with pericyte loss and acellular capillary formation, while in kidney it is associated with glomerular capillary loss in anti-glomerular basement membrane glomerulonephritis (9). A mechanistic link between elevated angiopoietin-2 levels and vascular pathology is suggested by the finding that Ang-2 can function as an autocrine regulator of endothelial inflammatory responses (12). These observations led us to hypothesize that hyperglycemia-induced methylglyoxal formation might directly regulate transcription of genes involved in diabetic vascular disease, such as Ang-2, by covalently modifying proteins that bind to the *Ang-2* promoter.

In the present study, we demonstrate that in mouse kidney microvascular endothelial cells increased glycolytic flux causes increased methylglyoxal modification of the corepressor mSin3A. Methylglyoxal modification of mSin3A results in increased recruitment of *O*-GlcNAc-transferase to an mSin3A-Sp3 complex, with consequent increased modification of Sp3 by *O*-linked *N*-acetylglucosamine. This modification of Sp3 causes decreased binding of the repressor complex to a glucose-

* This work was supported by grants from the National Institutes of Health and the Juvenile Diabetes Research Foundation. The costs of publication of this article were defrayed in part by the payment of page charges. This article must therefore be hereby marked "*advertisement*" in accordance with 18 U.S.C. Section 1734 solely to indicate this fact.

[S] The on-line version of this article (available at http://www.jbc.org) contains supplemental Figs. S1–S4.

[1] Both authors contributed equally to this work.

[2] To whom correspondence should be addressed. Tel.: 718-430-3636; Fax: 718-430-8570; E-mail: brownlee@aecom.yu.edu.

[3] The abbreviations used are: MG, methylglyoxal; Ang-2, angiopoietin-2; GLO1, glyoxalase 1; ICAM-1, intracellular adhesion molecule-1; *O*-GlcNAc, *O*-linked *N*-acetylglucosamine; OGT, *O*-GlcNAc-transferase; SOD2, manganese superoxide dismutase; TNF-α, tumor necrosis factor α; UCP-1, uncoupling protein-1; VCAM-1, vascular cell adhesion molecule-1; MKEC, murine kidney endothelial cell; IP, immunoprecipitation; aa, amino acid; WT, wild type.

responsive GC-box in the *Ang-2* promoter, resulting in increased *Ang-2* expression. High glucose-induced Ang-2 increased expression of intracellular adhesion molecule 1 (*ICAM-1*) and vascular cell adhesion molecule 1 (*VCAM-1*) both in cultured cells and in diabetic mice and sensitized microvascular endothelial cells to the proinflammatory effects of tumor necrosis factor α (TNF-α). This novel mechanism for regulating gene expression may play a role in the pathobiology of diabetic vascular disease.

EXPERIMENTAL PROCEDURES

Materials and Methods—Mouse *Ang-2* reporter plasmid (pGL3-mANG-2 (short)-Luc) was kindly provided by Drs. G. D. Yancopoulos and P. C. Maisonpierre. The related deletion promoter constructs were generated by PCR methods, and the indicated mutations were generated using the site-directed mutagenesis kit from Promega (Madison, WI). Rat *UCP-1* cDNA was provided by D. Ricquier (CNRS-Unite Propre 1511, Meudon, France), human *SOD2* cDNA was provided by L. Oberly (University of Iowa, Iowa City, IA), and human glyoxalase-I (*GLO1*) cDNA was provided by Dr. K. D. Tew (University of South Carolina, Charleston, S.C.). These cDNAs were cloned into the shuttle vector pAd5/CMV/K-NpA, and adenoviral vectors were prepared by the Gene Transfer Vector Core (University of Iowa). Mouse Gal4mSin3A was obtained from Dr. R. M. Evans. Rat *O*-GlcNAc-transferase (*OGT*) cDNA was obtained from G. W. Hart. pcDNA3 Gal4-AD-msin3A (mouse) and pVP16-mSin3A (888–955)/925 + 938(Q) double mutants were digested and ligated into Mfe1/XbaI sites for construction of Gal4-msin3A/925 + 938(Q) full-length double mutants. Detailed information regarding each construct is available upon request.

Murine *Ang-2* small interfering RNA (number 162193) was from Ambion. Ang-2 antibody (ab8452) was from Abcam (Cambridge, MA). GLO1 rabbit polyclonal antibody was produced and characterized by P. J. T. A monoclonal antibody to the major intracellular methylglyoxal-derived epitope, *N*α-acetyl-*N*δ (5-hydro-5-methyl)-4-imidazolone (M. G.), was generated and characterized by M. B., I. G., and P. J. T. Antibodies for Sp1, Sp3, mSin3A, and Gal4 were obtained from Santa Cruz Biotechnology. OGT rabbit polyclonal antibody (AL28) was kindly provided by Dr. G. W. Hart. *O*-GlcNAc monoclonal antibody (MA1–072) was purchased from Affinity BioReagents, Golden, CO.

The murine conditionally transformed kidney endothelial cell (MKEC) line was obtained from H-2K^b-tsA58 mice (13) and maintained in Dulbecco's modified Eagle's medium with 10% fetal bovine serum and antibiotics supplemented with essential amino acids and vitamins. Cells were grown at 33 °C, but experiments and treatment were performed at the nonpermissive temperature of 37 °C. Conditionally transformed human aortic endothelial cells were obtained from Dr. Anita Sumaga, Albert Einstein College of Medicine.

Plasmid DNA and small interfering RNA were transfected by Lipofectamine™ reagent (Invitrogen). Luciferase activity assays were carried out using the Dual-Luciferase™ Assay System (Promega), and transfection efficiencies were normalized using a cotransfected *Renilla* plasmid. Nuclear extracts were prepared using the NE-PER Nuclear and Cytoplasmic Extraction Reagents kit (Pierce Biotechnology). Protein concentration was measured by Coomassie Protein Assay kit (Pierce) using bovine serum albumin as a standard.

Reverse Transcription Reaction and Real-time Quantitative PCR—Total RNA from treated cells was extracted using the RNeasy Mini kit (Qiagen), and the RNA was reverse transcribed by SuperScript™ III First Strand Synthesis System (Invitrogen). Real-time quantitative PCR (qPCR) was run on a LightCycler Roche 480 (Roche Molecular Systems) with the LightCycler Roche 480 master kit. PCR was performed by denaturing at 95 °C for 5 min, followed by 45 cycles of denaturation at 95 °C, annealing at 60 °C, and extension at 72 °C for 10 s. Results were normalized by β-actin.

Immunoprecipitation (IP) and Western Blotting—Cell lysates or nuclear extracts were precleared by preimmune IgG plus Protein A-agarose beads for 2 h, and the supernatants were immunoprecipitated by the indicated antibodies and a 50% slurry of Protein A-agarose beads overnight at 4 °C (14). After washing with buffer containing 50 mM Tris, pH 7.5, 150 mM NaCl, 1% Nonidet P-40, and 0.5% deoxycholate with protease inhibitors, proteins were released and separated on 10% SDS-PAGE gels. The membranes were blotted by primary antibodies and then simultaneously incubated with the differentially labeled species-specific secondary antibodies anti-rabbit IRDye™ 800CW (green) and anti-mouse (or goat) Alexa Fluor 680 (red). Membranes were scanned and quantitated by the Odyssey Infrared Imaging System (LI-COR Biosciences).

Chromatin Immunoprecipitation—Treated cells were cross-linked by 1% formaldehyde for 20 min and terminated by addition of 0.1 M glycine. Cell lysates were sonicated and centrifuged. 500 μg of protein were precleared by bovine serum albumin/salmon sperm DNA plus preimmune IgG and a slurry of Protein A-agarose beads as previously described (14). Immunoprecipitations were performed with the indicated antibodies, bovine serum albumin/salmon sperm DNA, and a 50% slurry of Protein A-agarose beads. Input and immunoprecipitated DNA were washed and eluted and then incubated for 2 h at 42 °C in the presence of Proteinase K followed by 6 h at 65 °C to reverse the formaldehyde cross-linking. DNA fragments were recovered by phenol/chloroform extraction and ethanol precipitation. A 196-bp fragment from mice Ang-2 promoter (forward primer 5′-ccccctacaggaagatagtgg-3′ and reverse primer 5′-agctgtcctgagaggaaggag-3′) was amplified by real-time quantitative PCR.

Mammalian Two-hybrid Assays—The PAH4 domain of mouse *mSin3A* was amplified by PCR and subcloned into the Gal4-AD-pVP16 vector (Clontech). Indicated point mutations for mapping of the MG-responsive sites in the mSin3A PAH4 domain (aa 888–955) were prepared using the site-directed mutagenesis kit from Promega. Double mutants were prepared by BglII/Bfa I digestion and ligation of indicated fragments from pVP16-mSin3A (888–955) single mutants. The TPR 1–6 domain of OGT (aa 1–286) was amplified by PCR and subcloned into the Gal4-DBD-pM vector (Clontech). These plasmids and the pG5Luc reporter vector (Promega) were cotransfected into MKEC cells, and luciferase activity was measured by the Dual-Luciferase™ Assay System (Promega).

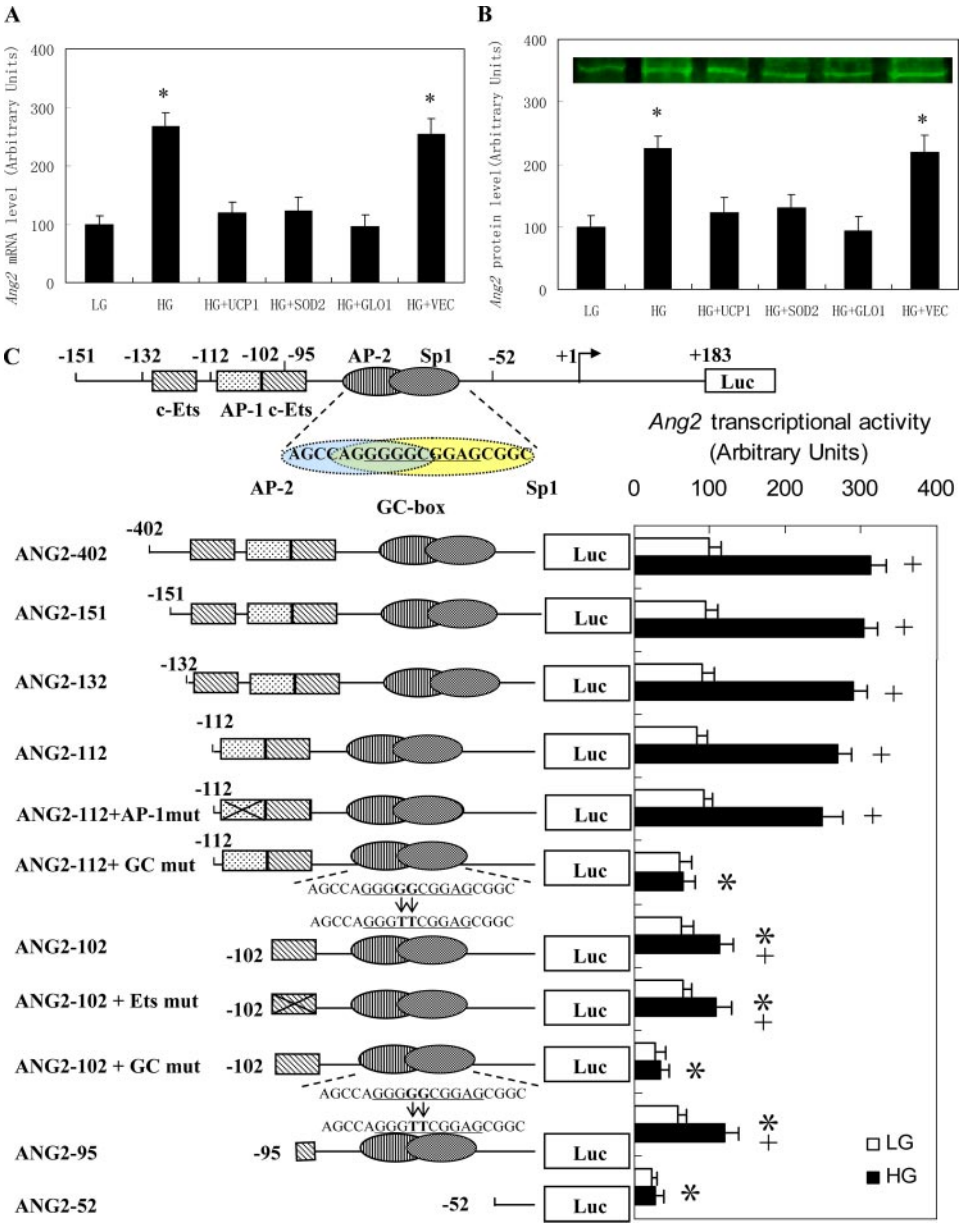

FIGURE 1. **Glyoxalase I overexpression prevents increased Ang-2 production induced by a glucose-responsive GC-box.** MKEC cells were incubated for 5 days in 5 mM glucose (*LG*), 30 mM glucose (*HG*), or HG after infection with UCP-1, SOD2, GLO1, or empty (*VEC*) adenoviral vectors. *A*, *Ang-2* mRNA was amplified and quantified by real-time quantitative PCR. *B*, Ang-2 protein was detected by Western blotting and quantified. *, $p < 0.01$ *versus* LG group. *C*, MKEC cells were transfected with the indicated *Ang-2* promoter reporter constructs and incubated in 5 mM (*LG*) or 30 mM (*HG*) glucose for 48 h, and *Ang-2* transcriptional activity was calculated from luciferase activity. *, $p < 0.01$ *versus* mAng-2 −402 HG. +, $p < 0.01$ *versus* mAng-2 −402 LG. Data are expressed as mean ± S.E. of three independent experiments.

In Vivo Mice Experiments—Chronic diabetic mice were induced by consecutive injection of 50 mg/kg streptozotocin (0.05 M sodium citrate, pH 5.5) for 5 days after an 8-h fasting. Animals with blood glucose >300 mg/dl are considered positive. Control mice received only vehicle injection. The mice were sacrificed by cervical dislocation prior to experiments. The kidney or other tissues were collected for further analysis of mRNA and protein level or the MG modification. All *in vivo* procedures were approved by the Institutional Animal Care and Use Committee.

Statistics—Results are given as mean ± S.E. All experiments were performed at least in triplicate. Data distribution was analyzed, and statistical differences for different treatments were evaluated by analysis of variance and the Tukey-Kramer test using SPSS 15 software.

RESULTS

Ang-2 Transcription Is Induced by High Glucose—Because incubation in high glucose increases intracellular glucose flux and methylglyoxal concentration in cells damaged by hyperglycemia (15), we first examined the effects of incubating MKEC cells in 30 mM glucose. This treatment increased *Ang-2* mRNA levels more than 2.7-fold compared with 5 mM glucose (Fig. 1*A*) and increased Ang-2 protein levels by 2.2-fold (Fig. 1*B*). Incubation in 30 mM mannitol, an osmotic control, did not (data not shown). Because overproduction of superoxide by mitochondria is the major mechanism by which high glucose increases intracellular levels of the glyoxalase I substrate methylglyoxal (15), we also evaluated the effect of overexpressing either uncoupling protein-1 (UCP-1), a specific protein uncoupler of oxidative phosphorylation capable of collapsing the proton electrochemical gradient, or manganese superoxide dismutase (SOD2), the mitochondrial form of this antioxidant enzyme. Each of these completely prevented the high glucose-induced increase of *Ang-2* mRNA and protein. (Fig. 1, *A* and *B*). Overexpression of GLO1, like UCP-1 and SOD2, completely prevented the high glucose-induced increase of *Ang-2* mRNA and protein in MKECs.

Identification of a Glucose-responsive Element in the Ang-2 Promoter—To localize the regulatory elements required for transcriptional activation of the *Ang-2* gene by high glucose, progressive 5′-promoter deletion constructs were generated containing different portions of the murine *Ang-2* promoter. In 5 mM glucose, the reporter activities were not markedly different among the −2239, −1921, −1221, −931, −677, −402, and −151 deletion constructs (numbered according to Ensembl Transcript ID: ENSMUST00000033846). In 30 mM glucose, activities were increased ~2.9-fold compared with those in 5 mM glucose in all constructs (data not shown). However, a significant decrease of activity was observed in the −52 construct compared with the

−151 construct in 5 mM glucose, and activity was not increased by high glucose. These data indicated that promoter elements between −151 and −52 are responsible for high glucose-induced transcriptional activation of the *Ang-2* promoter. Comparison of these sequences with transcription factor databases (TFSEARCH) revealed two c-Ets sites (positions −131 and −102), an AP-1 site (−111), an AP-2 site (−82), and an Sp1 site (−77) (Fig. 1*C*). We next explored the possible involvement of these motifs on the high glucose-induced increase in transcriptional activity of the *Ang-2* promoter using a series of mutated or deleted *Ang-2* luciferase constructs. As shown in Fig. 1*C*, deletion of the distal c-Ets (position −131) did not decrease high glucose-induced transcriptional activation. Similarly, mutation of the AP-1 site (construct −112 + AP-1 mut), the proximal c-Ets site (position −102), or deletion of sequence upstream of nucleotide −95 (construct −95) also had no effect. In contrast, mutation of the GC-rich sequences between the AP-2 and Sp1 site (−112 + GC mut and −102 + GC mut) and deletion of sequence upstream of nucleotide −52 both caused complete inhibition of high glucose-induced activation. These data indicated that the GC-rich sequence between the AP-2 and Sp1 sites is required for glucose responsiveness of the *Ang-2* promoter.

Sp3 and Sp1 Binding to the Ang-2 Promoter Changes in Response to High Glucose—To determine which of these nuclear proteins binds to the GC-box site and what the effects of high glucose and glyoxalase I overexpression are in the context of native chromatin structure, chromatin immunoprecipitation analysis was performed using antibodies specific for the indicated cognate proteins shown in Fig. 2. After immunoprecipitation and reversal of the cross-linking, the endogenous *Ang-2* promoter was enriched by real-time PCR amplification using primers specific for the *Ang-2* GC-box site. The PCR product from Sp1 immunoprecipitation was increased 3.1-fold by 30 mM glucose compared with 5 mM glucose, and this increase was prevented by overexpression of GLO1, as well as by overexpression of UCP-1 or SOD2 (Fig. 2*A*). In contrast, the PCR product from Sp3 chromatin immunoprecipitation was decreased 54% in 30 mM glucose compared with 5 mM (Fig. 2*B*). This decrease was prevented by overexpression of GLO1, as well as by overexpression of UCP-1 or SOD2. AP-2α binding was not affected by high glucose (Fig. 2*C*). These data indicated that Sp1, Sp3, and AP-2α bind to the *Ang-2* promoter in the context of its native chromatin structure and suggested that the observed changes in Sp1 and Sp3 binding induced by incubating cells in 30 mM glucose might mediate high glucose-induced *Ang-2* expression.

Sp3 Complexes with Methylglyoxal-modified Proteins, but Neither Sp3 nor Sp1 Is Modified by Methylglyoxal—Because GLO1 overexpression prevented high glucose-induced changes in Sp1 and Sp3 binding to the glucose-responsive element in the *Ang-2* promoter (Fig. 2), we hypothesized that high glucose induced these changes by modifying either Sp1, Sp3, or both with methylglyoxal. Surprisingly, however, when Sp1 and Sp3 were immunoprecipitated and then immunoblotted with anti-MG, neither protein was modified by MG (data not shown).

In contrast, when nuclear extracts from MKECs were immunoprecipitated with anti-MG antibody and immunoblotted for

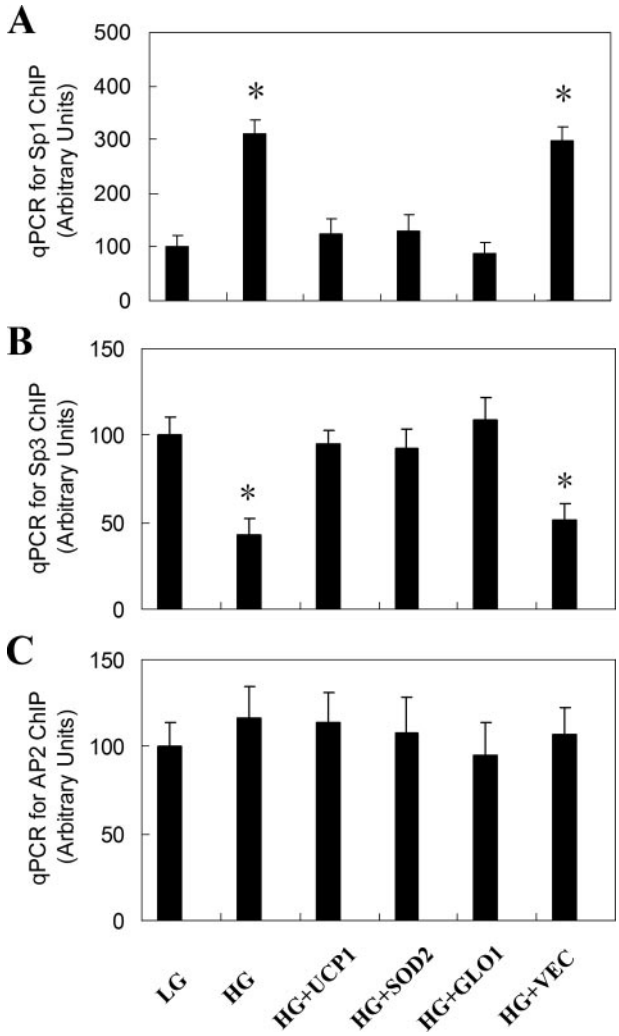

FIGURE 2. **High glucose decreases binding of Sp3 and increases binding of Sp1 to the *Ang-2* promoter *in vivo*.** MKEC cells were incubated as described in Fig. 1. Soluble chromatin was prepared from MKEC cells, followed by immunoprecipitation with antibodies to Sp1, Sp3, and AP-2α. The DNA extracted from the respective immunoprecipitates was amplified by real-time quantitative PCR (*qPCR*) using primers that amplify the glucose-responsive element in the mouse *Ang-2* promoter. qPCR results are shown for chromatin immunoprecipitation using antibodies to Sp1 (*A*), Sp3 (*B*), and AP2α (*C*). Data are expressed as mean ± S.E. of three independent experiments. *, $p < 0.01$ *versus* LG group.

Sp1 and Sp3, high glucose increased the density of the Sp3 band and GLO1 overexpression prevented this increase. The high glucose-induced increase in Sp3 band density was also prevented by overexpression of UCP-1 and SOD2 (Fig. 3*A*). Neither high glucose nor GLO1 overexpression affected Sp1 band density. These results suggested that an Sp3-associated protein was modified by methylglyoxal, rather than Sp3 itself, and that this modification might alter Sp3 binding to the *Ang-2* promoter.

Methylglyoxal Modifies mSin3A, Which Increases Its Association with OGT—Because a variety of proteins have been reported to associate with Sp3, we performed IP Western blots for HDAC1/2, RbAp46/48, N-CoR, OGT (data not shown), and mSin3A. Only the corepressor mSin3A was modified by MG (Fig. 3, *A* and *B*). Cells incubated in high glucose had a 2.1-fold increase in MG modification of mSin3A. Overexpression of

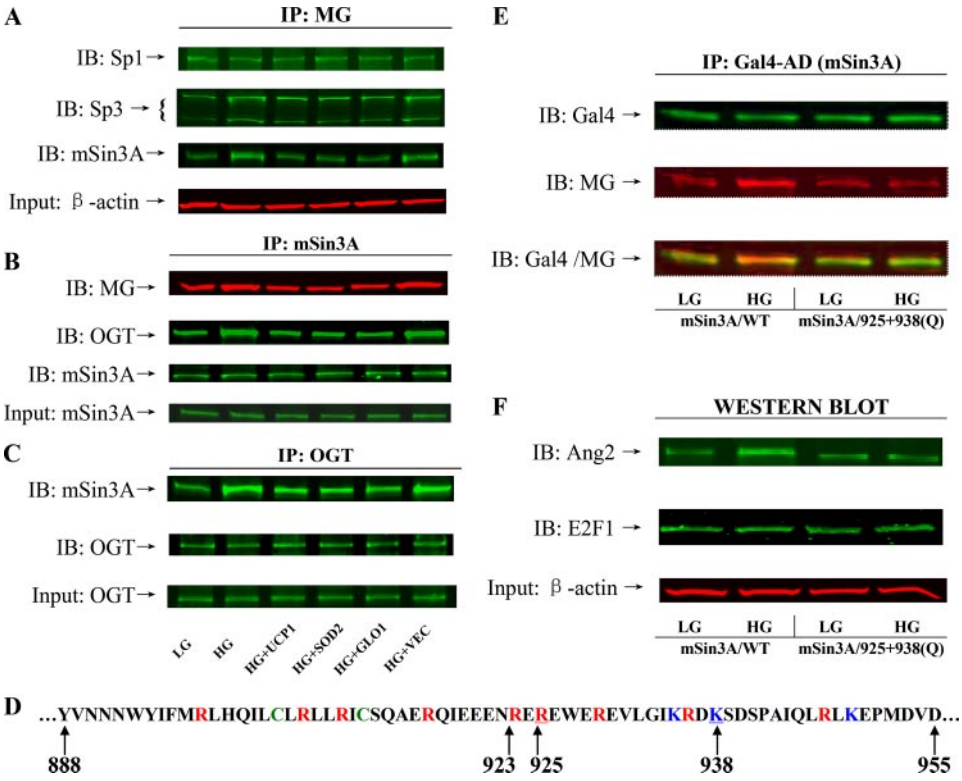

FIGURE 3. **Glucose-derived methylglyoxal modifies mSin3A at Arg-925 and Lys-938, which increases its association with OGT.** MKEC cells were incubated as described in Fig. 1. *A*, nuclear extracts were immunoprecipitated (*IP*) with antibodies to the major intracellular methylglyoxal-derived epitope, *Nα*-acetyl-*Nδ*-(5-hydro-5-methyl)-4-imidazolone (*MG*) and immunoblotted (*IB*) with antibodies to Sp1, Sp3, and mSin3A. *B*, nuclear extracts were immunoprecipitated (*IP*) with antibodies to mSin3A and immunoblotted (*IB*) with antibodies to MG, OGT, or mSin3A. *C*, nuclear extracts were immunoprecipitated (*IP*) with antibodies to OGT and immunoblotted (*IB*) with antibodies to mSin3A or OGT. 10% of cell lysates (for *β*-actin) or nuclear extracts (for mSin3A or OGT) were immunoblotted (*IB*) as input. *D*, amino acid sequence for mouse mSin3A PAH4 domain (aa 888–955). Potential MG-responsive sites are colored *red* for arginine (*R*), *blue* for lysine (*K*), and *green* for cysteine (*C*). *E*, MKEC cells were transfected with either wild type mouse Gal4-mSin3A (*mSin3A/WT*) or mSin3A double mutants (*mSin3A/925 + 938(Q)*) and incubated in either LG or HG for 5 days. The cell lysates were immunoprecipitated for Gal4-msin3A and then immunoblotted for Gal4 and MG. *F*, cells treated as described for *panel E*, above, were immunoblotted for Ang-2 and E2F1, with *β*-actin as input control.

GLO1, as well as UCP-1 and SOD2, prevented this increase. mSin3A has been reported to recruit the enzyme OGT (16). When immunoprecipitated mSin3A was immunoblotted for OGT, cells incubated in high glucose had significantly more OGT associated with mSin3A (Fig. 3*B*). Overexpression of GLO1, as well as UCP-1 and SOD2, prevented this increase. This effect was confirmed by immunoprecipitating OGT and then immunoblotting for mSin3A (Fig. 3*C*).

To determine which MG-modifiable residues in mSin3A were required for this increased binding of OGT, we first showed that the PAH4 domain of mSin3A was both necessary and sufficient for this methylglyoxal-responsive recruitment by subcloning different mSin3A domains (aa 1–189 (PAH1), aa 189–383 (PAH2), aa 383–526 (PAH3), aa 526–888 (HID), aa 888–955 (PAH4), and aa 955–1219 into the pVP16-AD-vector for mammalian two-hybrid assays with pM-DBD-OGT (1–286) (data not shown). These data are consistent with data reported by Yang *et al.* (16) showing that the PAH4 domain of mSin3A was necessary and sufficient for binding OGT. Although methylglyoxal reacts primarily with Arg residues *in vivo*, Lys and Cys residues in proteins can also be modified (17, 18). We therefore evaluated the possible role of each Arg, Lys, and Cys residue in the PAH4 domain of mSin3A (Fig. 3*D*) by making point mutants in the PAH4 domain that converted each of the 14 residues to glutamine. Mammalian two-hybrid assays showed that overexpression of GLO1 completely prevented the increased association of mSin3A with OGT induced by high glucose (data not shown). Single mutations of Arg-923, Arg-925, and Lys-938 partly prevented the increased association of mSin3A and OGT, and double mutation of Arg-925 and Lys-938 completely prevented the increased association. Double mutation of Arg-923 and Arg-925 was no more effective than mutation of Arg-925 alone, and double mutation of Arg-923 and Lys-938 was slightly more effective than mutation of Lys-938 alone (data not shown). These results are consistent with receptor binding domain analysis from the PAH4 domain sequence data (data not shown) that identified 6 methylglyoxal-modifiable residues as potential sites critical for protein-protein interaction (Arg-916, Arg-923, Arg-925, Arg-936, Arg-947, and Lys-938).

The effect of the double mutation on high glucose-induced modification of mSin3A by methylglyoxal was evaluated directly by IP:Western blot after overexpression of either WT or mutant mSin3A (Fig. 3*E*). Incubation in high glucose caused a 2.3-fold increase in MG modification of full-length WT mSin3A. In contrast, the double mutant mSin3A/925 + 938(Q) showed no increase in MG modification induced by incubation in high glucose. Using a two-color infrared fluorescent detection system, mSin3A and MG immunoreactivity were shown to co-localize. Loss of functionality of the mSin3A double mutant was demonstrated by identical experiments in which the effect of high glucose on *Ang-2* expression was assessed (Fig. 3*F*). High glucose incubation of cells overexpressing WT mSin3A increased Ang-2 expression by 2.1-fold, whereas high glucose incubation of cells overexpressing mSin3A/925 + 938 (Q) had no effect on Ang-2 expression. Bar graphs showing quantification across replicates for Fig. 3, *A–C*, *E*, and *F* are presented in supplemental Fig. S1. To determine whether this mechanism is common to other cell type-relevant diabetic complications, we repeated the experiments shown in Fig. 3, *E* and *F*, in human aortic endothelial cells (supplemental Fig. S2) and in retinal Muller cells (data not shown). In both cell types, exposure to high glucose increased Ang-2 production through methylglyoxal modification of mSin3A.

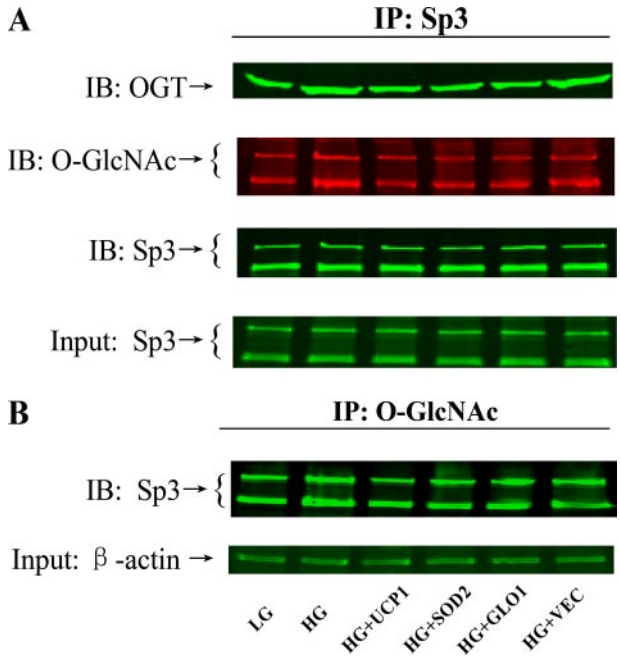

FIGURE 4. **Glyoxalase I overexpression prevents increased association of Sp3 with OGT and consequent increased modification of Sp3 by *O*-GlcNAc.** MKEC cells were incubated as described in Fig. 1. *A*, nuclear extracts were immunoprecipitated (*IP*) with antibodies to Sp3 and immunoblotted (*IB*) with antibodies to OGT or *O*-GlcNAc-modified protein. *B*, nuclear extracts were immunoprecipitated (*IP*) with antibodies to *O*-GlcNAc and immunoblotted (*IB*) with antibody to Sp3. 10% of cell lysates (*β-actin*) or nuclear extracts (for *Sp3*) were immunoblotted as input.

Association of Sp3 with OGT Causes Sp3 Glycosylation—To directly demonstrate that increased methylglyoxal induced by high glucose caused increased association of Sp3 with OGT, nuclear extracts were immunoprecipitated with anti-Sp3 and then immunoblotted for OGT and *O*-GlcNAc (Fig. 4*A*). High glucose increased association of Sp3 with OGT and also increased modification of Sp3 by *O*-GlcNAc. Overexpression of GLO1, as well as UCP-1 and SOD2, prevented both of these increases. These results were confirmed by immunoprecipitation with anti-*O*-GlcNAc and immunoblotting for Sp3 (Fig. 4*B*). Bar graphs showing quantification across replicates for Fig. 4, *A* and *B*, are presented in supplemental Fig. S3.

High Glucose-induced Ang-2 Increases ICAM-1 and VCAM-1 Expression in Both Cultured Cells and in Diabetic Mice—To determine whether the levels of Ang-2 induced in MKEC cells by high glucose were sufficient to induce expression of proinflammatory adhesion molecules in an autocrine fashion (12), we measured levels of *ICAM-1* and *VCAM-1* mRNA and protein. As shown in Fig. 5, high glucose increased *ICAM-1* (Fig. 5*A*) and *VCAM-1* (Fig. 5*B*) mRNA levels (2.1- and 1.7-fold, respectively) and protein levels (1.8- and 1.6-fold, respectively in Fig. 5*C*). Low concentrations of mice TNF-α had no effect on *ICAM-1* and *VCAM-1* expression when MKECs were incubated in 5 mM glucose. However, the same concentration of mTNF-α further increased *ICAM-1* and *VCAM-1* expression in MKECs incubated in 30 mM glucose, as shown in Fig. 5, *A* and *B*, for mRNA levels (3.3- and 3.7-fold, respectively), and protein levels (2.6- and 2.4-fold, respectively) in Fig. 5*C*. The effects of high glucose, both alone and in combination with TNF-α, were completely prevented by pretreatment with *Ang-2* small interfering RNA. These data indicate that high glucose-induced Ang-2 is sufficient to sensitize microvascular endothelial cells to the proinflammatory effects of TNF-α.

To determine whether these mechanisms are implicated in an *in vivo* model of diabetic nephropathy, kidneys were obtained from 5-month streptozotocin diabetic and age-matched C57Blk6 mice. As shown in Fig. 5*D*, mRNA levels of *Ang-2*, *ICAM-1*, and *VCAM-1* increased 1.7-, 2.3-, and 1.9-fold, respectively. Corresponding protein levels increased 1.4-, 1.8-, and 2.1-fold, respectively (Fig. 5*E*). mSin3A modification by MG was increased 1.7-fold in kidneys from diabetic mice compared with WT (Fig. 5*F*). Bar graphs showing quantification across replicates for Fig. 5, *C* and *F*, are presented in supplemental Fig. S4.

DISCUSSION

In the present study, we describe a novel mechanism for regulation of gene expression by high glucose: coregulatory protein modification by the glycolysis-derived dicarbonyl metabolite methylglyoxal. We demonstrate that in mouse kidney endothelial cells, increased glycolytic flux causes increased methylglyoxal modification of the corepressor mSin3A. Methylglyoxal modification of mSin3A results in increased recruitment of *O*-GlcNAc-transferase to an mSin3A-Sp3 complex, with consequent increased modification of Sp3 by *O*-linked *N*-acetylglucosamine. This modification of Sp3 causes decreased binding to a glucose-responsive GC-box in the angiopoietin-2 promoter, resulting in increased *Ang-2* expression. High glucose-induced Ang-2 increased expression of *ICAM-1* and *VCAM-1* in both cultured cells and kidneys from diabetic mice and sensitized microvascular endothelial cells to the proinflammatory effects of TNF-α. In human aortic endothelial cells and in retinal Muller cells, the major cell type expressing angiopoietin-2 in the retina (19), high glucose-induced Ang-2 expression is also mediated by this mechanism[4] (supplemental Fig. 2).

mSin3A has been shown to recruit the enzyme OGT to promoters in several tumor cell lines, which then acts in concert with histone deacetylation to promote gene silencing (16). In contrast, our data in mouse kidney endothelial cells and in retinal Muller cells show that recruitment of OGT to mSin3A activates, rather than represses, gene expression when the mSin3A is modified by methylglyoxal arising from high glucose flux and reactive oxygen species formation by the mitochondrial electron transport chain. mSin3A binding with the ubiquitous transcription factor Sp3 has not been reported previously. Sp3 and Sp1 compete for common GC-rich target sequences in promoter elements (20, 21). Although both Sp3 and Sp1 may act as inhibitors or activators of gene expression, Sp3 has been found to repress Sp1-mediated transcriptional activation in a number of cell types (22, 23). *O*-GlcNAcylation of Sp1 may stimulate or repress transcription (24–27), most likely depending on which residues are modified. In 293 cells and SL2 cells, Sp3 was not modified by *O*-GlcNAc, as determined by wheat germ agglutinin affinity chromatography (28).

[4] P. Scherer, personal communication.

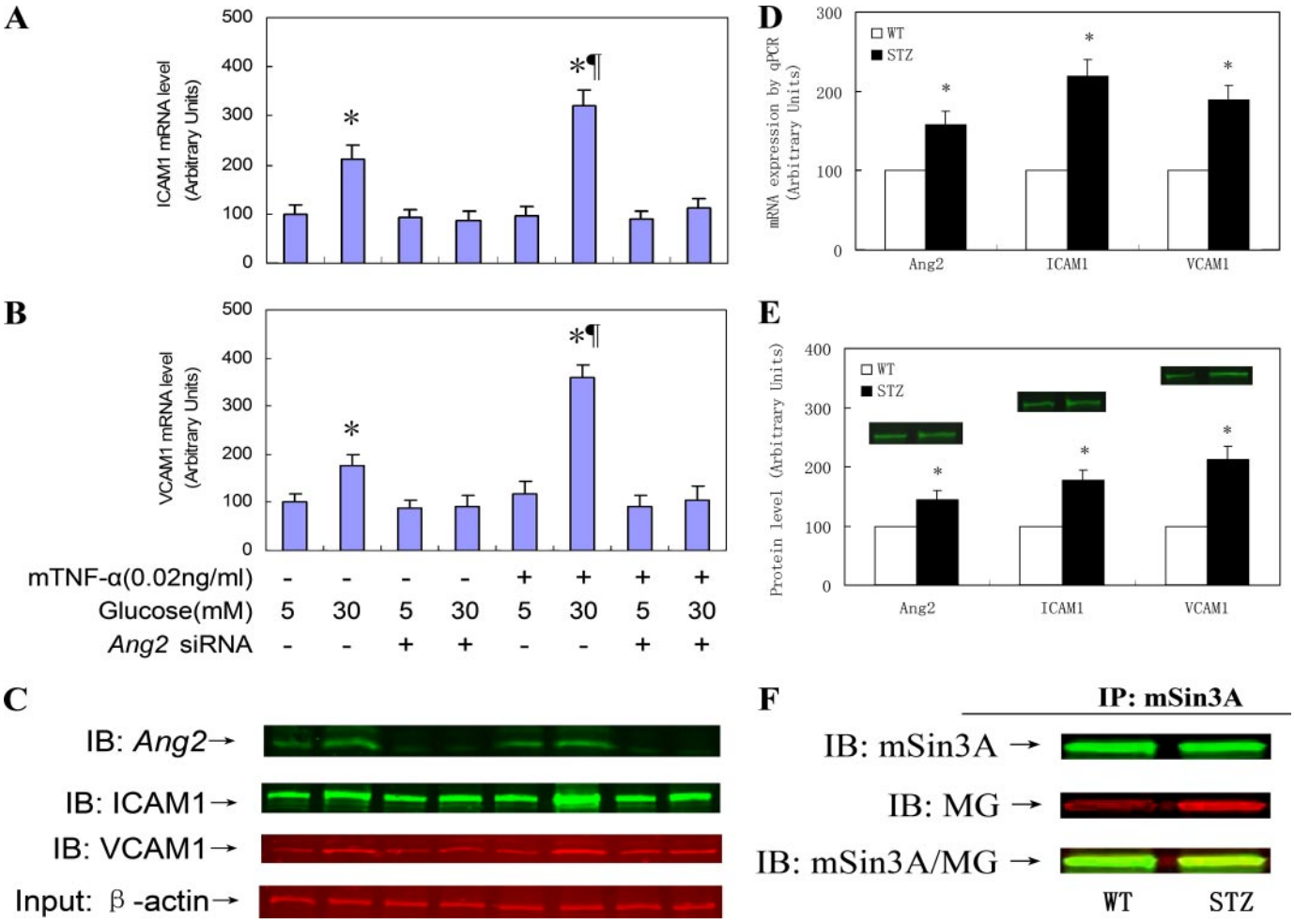

FIGURE 5. **High glucose-induced Ang-2 increases ICAM-1 and VCAM-1 expression both *in vitro* and *in vivo*.** *A*, MKEC cells were incubated in LG and HG, alone or after transfection with Ang-2 small interfering RNA. Cells were incubated in the absence or presence of mTNF-α (0.02 ng/ml) for 4 h and then harvested for analysis of *ICAM-1* mRNA levels (*A*), analysis of *VCAM-1* mRNA levels (*B*), and Ang-2, ICAM-1, and VCAM-1 protein levels (*C*) by Western blot. 10% of cell lysates was blotted for β-actin as input control. *, $p < 0.01$ *versus* 5 mM glucose group; ¶, $p < 0.01$ *versus* 30 mM glucose group. *D–F*, age-matched control (*WT*) and streptozotocin-induced diabetic mice were sacrificed and kidneys were analyzed for *Ang-2*, *ICAM-1*, and *VCAM-1* mRNA levels (*D*), Ang-2, ICAM-1, and VCAM-1 protein levels (*E*), and for mSin3A modification by MG (*F*). *, $p < 0.01$ *versus* WT group, $n = 4$.

However, the effect of increased glucose flux on *O*-GlcNAc modification of Sp3 was not evaluated.

Regulation of gene expression involves complex interactions among histones, transcription factors, coactivators, and corepressors. An emerging concept is that coactivator and corepressor proteins may be primary targets of physiologic signals, coordinating distinct biological programs (29). Post-translational modifications of coactivator proteins have been described (30, 31) that are thought to regulate coactivator function. Our studies demonstrate for the first time that methylglyoxal causes post-translational modification of a coregulator protein and that this modification affects gene expression. The extent of this modification reflects the net effect of a variety of intracellular processes, including metabolic flux and reactive oxygen formation, and may thus function as a new integrating signal to coordinately regulate distinct patterns of gene expression. The specific increase in Ang-2 expression by this mechanism in response to high glucose has important implications for understanding the pathogenesis of diabetic complications. High glucose-induced Ang-2 increased expression of *ICAM-1* and *VCAM-1* both in cultured cells and in kidneys from diabetic mice and sensitized microvascular endothelial cells to the proinflammatory effects of TNF-α. TNF-α is elevated in both kidney and retina of diabetic animals, and both experimental diabetic nephropathy and retinopathy are significantly attenuated in *ICAM-1* knock-out mice (32–35). Pharmacologic agents that reduce methylglyoxal concentration in cells susceptible to diabetic complications may have important clinical benefits.

REFERENCES

1. Phillips, S. A., and Thornalley, P. J. (1993) *Eur. J. Biochem.* **212,** 101–105
2. Richard, J. P. (1993) *Biochem. Soc. Trans.* **21,** 549–553
3. Thornalley, P. J. (2003) *Biochem. Soc. Trans.* **31,** Pt. 6, 1343–1348
4. Ahmed, N., and Thornalley, P. J. (2003) *Biochem. Soc. Trans.* **31,** Pt. 6, 1417–1422
5. Hammes, H. P., Du, X., Edelstein, D., Taguchi, T., Matsumura, T., Ju, Q., Lin, J., Bierhaus, A., Nawroth, P., Hannak, D., Neumaier, M., Bergfeld, R., Giardino, I., and Brownlee, M. (2003) *Nat. Med.* **9,** 294–299
6. Karachalias, N., Babaei-Jadidi, R., Ahmed, N., and Thornalley, P. J. (2003) *Biochem. Soc. Trans.* **31,** Pt. 6, 1423–1425
7. Du, X., Matsumura, T., Edelstein, D., Rossetti, L., Zsengeller, Z., Szabo, C., and Brownlee, M. (2003) *J. Clin. Investig.* **112,** 1049–1057
8. Hammes, H. P., Lin, J., Wagner, P., Feng, Y., Vom Hagen, F., Krzizok, T.,

Renner, O., Breier, G., Brownlee, M., and Deutsch, U. (2004) *Diabetes* **53,** 1104–1110
9. Yuan, H. T., Tipping, P. G., Li, X. Z., Long, D. A., and Woolf, A. S. (2002) *Kidney Int.* **61,** 2078–2089
10. Singh, A. K., Gudehithlu, K. P., Pegoraro, A. A., Singh, G. K., Basheerudin, K., Robey, R. B., Arruda, J. A., and Dunea, G. (2004) *Lab. Investig.* **84,** 597–606
11. Rizkalla, B., Forbes, J. M., Cao, Z., Boner, G., and Cooper, M. E. (2005) *J. Hypertens.* **23,** 153–164
12. Fiedler, U., Reiss, Y., Scharpfenecker, M., Grunow, V., Koidl, S., Thurston, G., Gale, N. W., Witzenrath, M., Rosseau, S., Suttorp, N., Sobke, A., Herrmann, M., Preissner, K. T., Vajkoczy, P., and Augustin, H. G. (2006) *Nat. Med.* **12,** 235–239
13. Langley, R. R., Ramirez, K. M., Tsan, R. Z., Van Arsdall, M., Nilsson, M. B., and Fidler, I. J. (2003) *Cancer Res.* **63,** 2971–2976
14. Metivier, R., Penot, G., Hubner, M. R., Reid, G., Brand, H., Kos, M., and Gannon, F. (2003) *Cell* **115,** 751–763
15. Brownlee, M. (2001) *Nature* **414,** 813–820
16. Yang, X., Zhang, F., and Kudlow, J. E. (2002) *Cell* **110,** 69–80
17. Van Herreweghe, F., Mao, J., Chaplen, F. W., Grooten, J., Gevaert, K., Vandekerckhove, J., and Vancompernolle, K. (2002) *Proc. Natl. Acad. Sci. U. S. A.* **99,** 949–954
18. Chaplen, F. W., Fahl, W. E., and Cameron, D. C. (1998) *Proc. Natl. Acad. Sci. U. S. A.* **95,** 5533–5538
19. Sarthy, V. P., Brodjian, S. J., Dutt, K., Kennedy, B. N., French, R. P., and Crabb, J. W. (1998) *Investig. Ophthalmol. Vis. Sci.* **39,** 212–216
20. Suske, G. (1999) *Gene* **238,** 291–300
21. Li, L., He, S., Sun, J. M., and Davie, J. R. (2004) *Biochem. Cell Biol.* **82,** 460–471
22. Hagen, G., Muller, S., Beato, M., and Suske, G. (1994) *EMBO J.* **13,** 3843–3851
23. Ghayor, C., Chadjichristos, C., Herrouin, J. F., Ala-Kokko, L., Suske, G., Pujol, J. P., and Galera, P. (2001) *J. Biol. Chem.* **276,** 36881–36895
24. Roos, M. D., Su, K., Baker, J. R., and Kudlow, J. E. (1997) *Mol. Cell. Biol.* **17,** 6472–6480
25. Yang, X., Su, K., Roos, M. D., Chang, Q., Paterson, A. J., and Kudlow, J. E. (2001) *Proc. Natl. Acad. Sci. U. S. A.* **98,** 6611–6616
26. Kang, H. T., Ju, J. W., Cho, J. W., and Hwang, E. S. (2003) *J. Biol. Chem.* **278,** 51223–51231
27. Du, X. L., Edelstein, D., Rossetti, L., Fantus, I. G., Goldberg, H., Ziyadeh, F., Wu, J., and Brownlee, M. (2000) *Proc. Natl. Acad. Sci. U. S. A.* **97,** 12222–12226
28. Sapetschnig, A., Koch, F., Rischitor, G., Mennenga, T., and Suske, G. (2004) *J. Biol. Chem.* **279,** 42095–42105
29. Lin, J., Wu, P. H., Tarr, P. T., Lindenberg, K. S., St.-Pierre, J., Zhang, C. Y., Mootha, V. K., Jager, S., Vianna, C. R., Reznick, R. M., Cui, L., Manieri, M., Donovan, M. X., Wu, Z., Cooper, M. P., Fan, M. C., Rohas, L. M., Zavacki, A. M., Cinti, S., Shulman, G. I., Lowell, B. B., Krainc, D., and Spiegelman, B. M. (2004) *Cell* **119,** 121–135
30. Fingerman, I. M., and Briggs, S. D. (2004) *Cell* **117,** 690–691
31. Chakraborty, S., Senyuk, V., and Nucifora, G. (2001) *J. Cell. Biochem.* **82,** 310–325
32. Navarro, J. F., Milena, F. J., Mora, C., Leon, C., and Garcia, J. (2006) *Am. J. Nephrol.* **26,** 562–570
33. Chow, F. Y., Nikolic-Paterson, D. J., Ozols, E., Atkins, R. C., and Tesch, G. H. (2005) *J. Am. Soc. Nephrol.* **16,** 1711–1722
34. Krady, J. K., Basu, A., Allen, C. M., Xu, Y., LaNoue, K. F., Gardner, T. W., and Levison, S. W. (2005) *Diabetes* **54,** 1559–1565
35. Joussen, A. M., Poulaki, V., Le, M. L., Koizumi, K., Esser, C., Janicki, H., Schraermeyer, U., Kociok, N., Fauser, S., Kirchhof, B., Kern, T. S., and Adamis, A. P. (2004) *FASEB J.* **18,** 1450–1452

High Glucose Increases Angiopoietin-2 Transcription in Microvascular Endothelial Cells through Methylglyoxal Modification of mSin3A

Dachun Yao, Tetsuya Taguchi, Takeshi Matsumura, Richard Pestell, Diane Edelstein, Ida Giardino, Guntram Suske, Naila Rabbani, Paul J. Thornalley, Vijay P. Sarthy, Hans-Peter Hammes and Michael Brownlee

J. Biol. Chem. 2007, 282:31038-31045.
doi: 10.1074/jbc.M704703200 originally published online August 1, 2007
